

# Role of the carbon nanocoating on the electronic conductivity of LiFePO<sub>4</sub> based electrodes for lithium ion batteries

J.C. Badot<sup>\*</sup>, K.A. Seid<sup>\*\*</sup>, O. Dubrunfaut<sup>\*\*</sup>, S. Levasseur<sup>\*\*\*</sup>, B. Lestriez<sup>\*\*\*\*</sup>, and D. Guyomard<sup>\*\*\*\*</sup>

<sup>\*</sup>Laboratoire de Chimie de la Matière Condensée de Paris, Chimie-ParisTech, Univ Paris 06, CNRS, France, jc-badot@chimie-paristech.fr

<sup>\*\*</sup>Laboratoire de Génie Electrique de Paris, SUPELEC, UPMC Univ Paris 06, Univ Paris-Sud, CNRS, France,

<sup>\*\*\*</sup>UMICORE Cobalt & Specialty Materials, Belgium

<sup>\*\*\*\*</sup>Institut des Matériaux Jean Rouxel (IMN), Université de Nantes, CNRS, France

## ABSTRACT

Composite and nanostructured materials have hierarchical architecture with different levels: (a) macroscopic (substructure of porous clusters); (b) mesostructural (particles constituting the clusters); and (c) microscopic and nanometric (coatings, bulk of the particles). The identification of the key parameters that affect the electronic transport across all observed size scales is required, but is not possible using conventional dc-conductivity measurements. The broadband dielectric spectroscopy (BDS) from low-frequencies (few Hz) to microwaves (few GHz) is applied to one of the most important composite materials for lithium batteries. LiFePO<sub>4</sub> is wrapped in a carbon coating whose electrical properties, although critical for battery performance, have never been measured due to its nanometre-size and the powdery nature of the material.

**Keywords:** provide up to five comma separated, keywords for indexing, don't capitalize

## 1 INTRODUCTION

A lithium-ion battery also known as Li-ion battery or LiB is a family of rechargeable battery types using no lithium metal at the negative electrode in which lithium ions move from the negative electrode to the positive electrode during discharge, and back when charging. Chemistry, performance, cost, and safety characteristics vary across LiB types. Unlike lithium primary batteries (which are disposable), lithium-ion electrochemical cells use an intercalation lithium compound as the electrode material instead of metallic lithium. Lithium-ion batteries are common in consumer electronics. They are one of the most popular types of rechargeable batteries for portable electronics, with one of the best energy densities, no memory effect, and a slow loss of charge when not in use. Beyond consumer electronics, LiBs are also growing in popularity for military, electric vehicle, and aerospace applications. Research is yielding a stream of improvements to traditional LiB technology, focusing on

energy density, durability, cost, and intrinsic safety. Positive and negative electrodes are however composite electrodes. The composite electrode is a very complex medium obtained by mixing together the active material (AM) grains with non-electro active additives such as a conducting agent (C) and a polymeric binder (B) For high rate performance this medium needs to bring very efficiently the ions and the electrons to the surface of the active material (AM) particles.

The resulting hierarchical architecture induces polarizations which are generally visible by the BDS [1] because they involve changes in local charge density. at the micro structural scale, a conducting polycrystalline material (compact powders, ceramics) presents interfacial polarizations. The interfaces are generally grain (particles) boundaries or more often, the contact area between the grains. If the grains (particles) are assembled into clusters (i.e. agglomerates), there exists a different interface between clusters. In addition, an interface exists between the sample and the electrodes contact (e.g., gold, silver) used for the measurement.

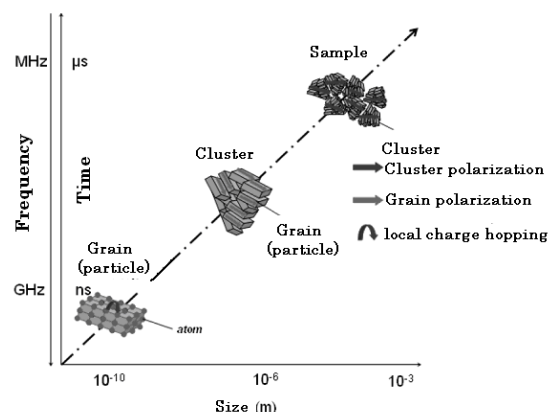


Figure 1. Multi-scale analysis of electric polarization in a conducting material [1]

These types of polarization are visible only at low frequencies. The characteristic frequencies of the different phenomena observed in dielectric spectroscopy are

classifiable according to the characteristic scale at which they are observed. Furthermore, the larger characteristic size the smaller the characteristic frequency is (Figure 2). The improvement in electronic conductivity of the composite electrode is crucial toward high rate performance. Our previous work demonstrated the critical role of the polymer binder and electrode morphology on the electronic conductivity of the composite electrode [1]. We also showed that the carbon black/binder network can be considered as a macro-tunnel junction, with an exponential drop of electronic conductivity as a function of the thickness of the binder nanolayer adsorbed at the contacts between the carbon black particles. However, the direct current (dc) transverse electronic conductivity (sample conductivity), that is the usually measured quantity, is a macroscopic averaged quantity.

## 2 EXPERIMENTAL

Complex resistivity and permittivity spectra were recorded over a broad frequency range 40 to  $10^{10}$  Hz, using simultaneously an impedance analyzer (Agilent 4294 from 40 to  $1.1 \times 10^8$  Hz) and a network analyzer (HP 8510 from  $4.5 \times 10^7$  to  $10^{10}$  Hz). The experimental device, fully described in previous paper [2], consists of a coaxial cell (APC7 standard) in which the cylindrically shaped sample with silver plated front faces, fills the gap between the inner conductor and a short circuit. The sample has the same diameter as (7 mm) that of the outer conductor of the coaxial cell. After a relevant calibration of the analyzers, the complex (relative) permittivity  $\epsilon(\omega) = \epsilon'(\omega) - i\epsilon''(\omega)$  of the sample is computed from its admittance  $Y_s$ . Complete dielectric spectra were made from about 400 measurements with an accuracy of approximately 3 to 5% in the experimental frequency range. The knowledge of the complex permittivity enables the calculation of the complex conductivity  $\sigma = \sigma' + i\sigma'' = i\omega\epsilon_0\epsilon(\omega)$  ( $\epsilon_0$  being the vacuum permittivity) and resistivity  $\rho = \sigma^{-1}$ .

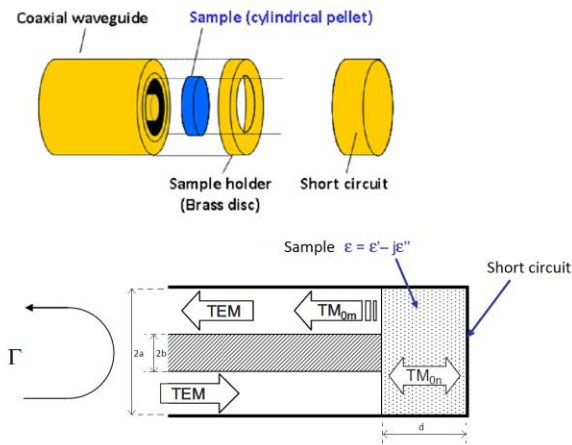


Figure 2. Schemes 3D and 2D of the measuring cell in a reflection mode.  $TM_{0n}$  or  $n$  are transverse magnetic waves

## 3 RESULTS AND DISCUSSION

The broadband dielectric spectroscopy (BDS) is well-known for ionic conductors and polymers but much less used for electronic conductors. We have applied this technique to the study of nanocomposites prepared from the most important active material for lithium batteries, cluster of  $LiFePO_4$  particles, coated in a core shell morphology with an amorphous carbon coating of few nanometres thick. Our objective was to extract the electronic conductivity of this nanocomposite at all the scales of its architecture (from inter atomic distances to macroscopic lengths), with the aim of identifying the limiting parameters and move on to systematic and rational manufacturing. Processing and engineering practices for the better. Binary systems ( $LiFePO_4$  with its carbon coating) were studied to establish the fundamental know-how on the electrical properties of the different scales and the existing correlation between the scales of a compacted powder.

The frequency dependence of the real parts of the conductivity  $\sigma$  and of the permittivity  $\epsilon'$  for  $LiFePO_4$  (LFP) and coated  $LiFePO_4$  (CLFP) is shown in Figure 3.

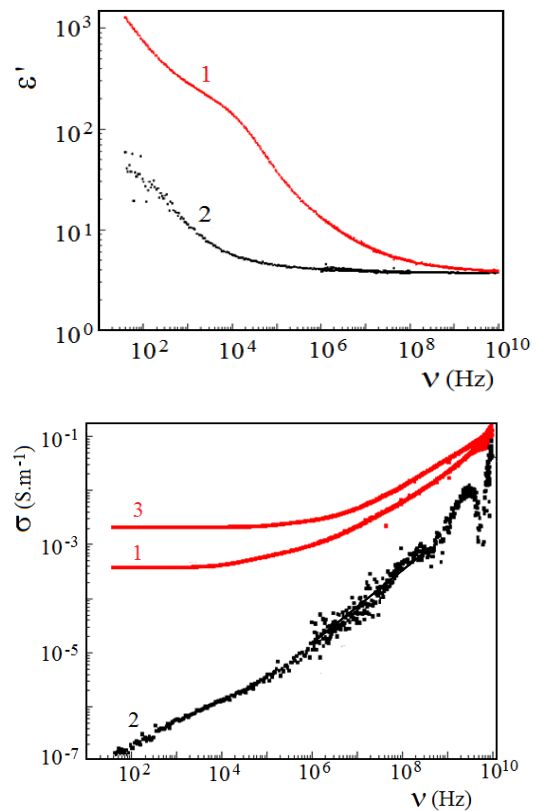


Figure 3. Real parts of the permittivity  $\epsilon'$  and the conductivity  $\sigma$  as functions of the frequency for both carbon-coated (CLFP at 300 and 400 K: curves 1 and 3) and uncoated (LFP at 300 K: curve 2) samples [3].

The carbon coating in CLFP drastically increases the electrical conductivity in the whole frequency range (Fig. 5). At 300 K, the dc-conductivity  $\sigma_s$  of the sample has a

value of more than  $10^{-4} \text{ S.m}^{-1}$  below  $10^5 \text{ Hz}$  and the high frequency conductivity reaches almost  $10^{-1} \text{ S.m}^{-1}$  in the GHz region. This type of frequency dependence shows that in the composite CCLFP, the carbon-coating constitutes continuous conducting paths spanning throughout the sample [3]. This situation can be realized with a small volume fraction of conductor owing to the core-shell morphology of the carbon-coated  $\text{LiFePO}_4$ .

The decomposition of the dielectric and resistivity spectra allows to evidenced some relaxations (absorption) due to polarization fluctuations and to the existence of contact resistances within the samples. The results obtained in this work demonstrate that the BDS can distinguish the different types of electronic transfers involved at the different scales of the material architecture. These phenomena occur from interatomic to macroscopic sizes with the influence of the morphology of the different constituents at these scales. Considering a composite material composed of an active material (e.g.  $\text{LiFePO}_4$ ) and a conductive agent (e.g. carbon coating), when the frequency increases, different kinds of polarizations, giving rise to dielectric relaxations, appear in following order: a) Space-charge polarization (low-frequency range) due to the interface between the sample and the conductive metallic layer deposited on it; b) Polarization of C- $\text{LiFePO}_4$  clusters (micronic and/or submicronic scales) due to the existence of resistive junctions between them; c) Electron hopping between  $\text{sp}^2$  domains (nanometric scale) within the carbon coating around the  $\text{LiFePO}_4$  particles.

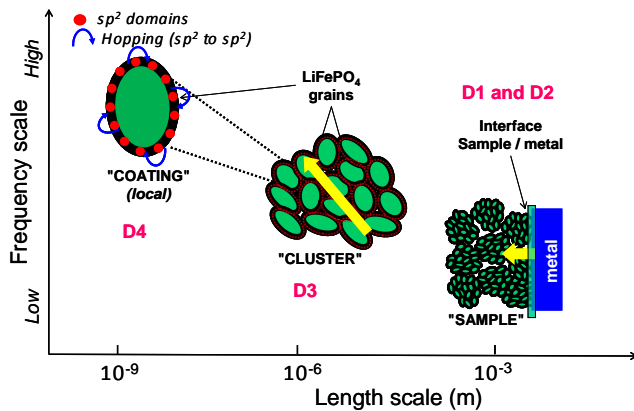


Figure 4. Schematic description of the hierarchical architecture within the CLFP samples giving rise to different sources of polarizations (interfacial, clusters, electron hopping in the coating) and contact resistances (sample-device, interclusters, interparticules) [3]

The conductivity and permittivity of the composites measured are effective parameters since they are functions of the relative concentration of the different phases. Using the Brick Layer Model and the General Effective Medium theory [4], it was possible to provide some orders of magnitude for the true values of the conductivity at the

different scales of the material (Fig. 5) 10), i.e. macroscopic, cluster, coating and  $\text{sp}^2$  domain levels.

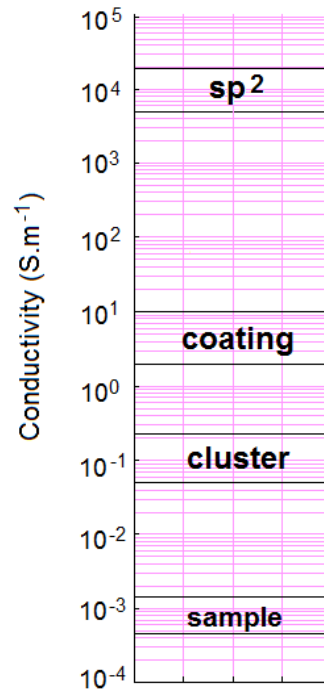


Figure 5. Schematic description of the hierarchical architecture within the samples giving rise to different sources of polarizations [3].

The major drop in conductivity is due to the presence of  $\text{sp}^3$  discontinuities in the coating that result in a loss of  $\sim 10^3$  when going from the  $\text{sp}^2$  domains to the coating scale. Although the carbon volume fraction in the CLFP cluster is very low (less than 5 %), the loss is only a factor of  $\sim 10$  when going from the coating to the cluster scale. Inter-cluster junctions result in another conductivity loss of  $\sim 10$ . The high activation energy for electrons transport associated with the  $\text{sp}^3$  discontinuities result in a large decrease of the conductivity with decreasing temperature, which is a drawback or limitation of the CCLFP material.

## 4 CONCLUSION

This work provided a new approach towards a fundamental understanding of the electrical properties of composites for lithium ion batteries. It also gave a new perspective on the quantitative relationships existing between the different scales. This relationships offer the opportunity to pin point the limiting scales and conductivity mechanisms. Which in turn will be instrumental to make adjustments on the whole process of the electrode material synthesis, processing, manufacturing, engineering and so on for the objective of addressing the inherent conductivity problems in the studied material.

## ACKNOWLEDGEMENTS

Financial funding from CNRS, UMICORE and the ANR program no. ANR-09-STOCK-E-02-01 is acknowledged.

## REFERENCES

- [1] J.C. Badot, E. Ligneel, O. Dubrunfaut, D. Guyomard and B. Lestriez, *Adv. Funct. Mater.* 19, 2749, 2009.
- [2] N.E. Belhadj-Tahar, A. Fourier-Lamer, *IEEETrans. Microwaves Theory and Tech.* 39(10), 1718, 1991.
- [3] K.A. Seid, J.C. Badot, O. Dubrunfaut, S. Levasseur, D. Guyomard and B. Lestriez, *J. Mater. Chem.* 22, 2641, 2012.
- [4] C. Chiteme, D.S. McLachlan, *Phys. B* 279, 69, 2000.